

11 Mar 1991, 2:30 pm - 3:30 pm

Flow Failure of Liquefied Sand in Large-Scale Shaking Tables

Kenji Ishihara
University of Tokyo, Japan

Mikio Takeuchi
Okumura Co., Japan

Follow this and additional works at: <https://scholarsmine.mst.edu/icrageesd>



Part of the [Geotechnical Engineering Commons](#)

Recommended Citation

Ishihara, Kenji and Takeuchi, Mikio, "Flow Failure of Liquefied Sand in Large-Scale Shaking Tables" (1991). *International Conferences on Recent Advances in Geotechnical Earthquake Engineering and Soil Dynamics*. 10.

<https://scholarsmine.mst.edu/icrageesd/02icrageesd/session14/10>



This work is licensed under a [Creative Commons Attribution-Noncommercial-No Derivative Works 4.0 License](#).

This Article - Conference proceedings is brought to you for free and open access by Scholars' Mine. It has been accepted for inclusion in International Conferences on Recent Advances in Geotechnical Earthquake Engineering and Soil Dynamics by an authorized administrator of Scholars' Mine. This work is protected by U. S. Copyright Law. Unauthorized use including reproduction for redistribution requires the permission of the copyright holder. For more information, please contact scholarsmine@mst.edu.



Flow Failure of Liquefied Sand in Large-Scale Shaking Tables

(State of the Art Paper)

Kenji Ishihara

Professor of Civil Engineering, University of Tokyo

Mikio Takeuchi

Civil Engineer, Okumura Co.

ABSTRACT Laboratory studies on flow failure in liquefied sand deposits using large-scale shaking tables are briefly introduced, together with a case study on the lateral deformation in the field. The key parameters influencing the occurrence of flow-type deformation are discussed in an effort to figure out a mechanism or scenario of the flow failure. In one series of the laboratory studies, shaking table tests were performed to examine the effectiveness of a preventive measure against the flow slide. This aspect is also discussed briefly.

INTRODUCTION

When liquefaction takes place in sandy deposits during earthquakes, the ground is known to often undergo a large amount of permanent deformation as a result of lateral flow of liquefied soils, even though the ground is nearly flat. In fact, large deformations as much as several meters are reported by Hamada et al. (1986) to have developed on slopes as flat as 0.5 % in the outskirts of Noshiro city during the Nihonkai-chubu earthquake of 1983 in Japan. This type of permanent deformation is considered to develop, during a period of small-intensity to none shaking following the main shock, due to the action of gravity-induced driving shear stress which is in excess of residual strength or steady-state strength of soils becoming available after the onset of cyclic softening or initial liquefaction. Thus, if the residual strength is small enough, the large deformation can develop in any ground conditions even if the driving shear stress is very small. Experiences in the recent earthquakes appear to indicate that there are three major ground conditions as follows in which the lateral flow can occur.

- 1) Flat ground in front of a surcharge such as dikes and embankments.
- 2) Flat ground behind the water front such as rivers, lakes and sea.
- 3) Slightly sloped ground.

There are several reported evidences of lateral flow having taken place during recent major earthquakes such as the 1948 Fukui earthquake in Japan (Hamada et al., 1989), the 1923 Kanto earthquake in Japan (Wakamatsu et al. 1989) and the 1971 San Fernando earthquake (O'Rourke et al. 1989). As a result of the case studies as above, it is known that the amount of permanent deformations in the liquefied sand deposits are generally on the order of several meters and they can develop over a wide area extending several tens of meters from the place where the lateral flow is initiated.

In view of the importance of the flow-type phenomenon, several attempts have been made to reproduce the liquefaction-induced flow failure in artificially prepared deposits using large-scale shaking tables in the laboratory, as well as by means of centrifuge shaking tests (Arulanandan et al 1988). Major efforts in Japan in this regard have been, however, to explore the mechanism of flow failure by means of large-scale shaking table tests.

In this paper, two of the major laboratory tests are introduced somewhat in details with reference to a case study in the field, and an attempt will be made to point out key parameters influencing the occurrence of flow type deformation. Once the flow is known to take place, of major concern is how to stop or to minimize its detrimental effects. Some laboratory tests were also conducted to examine effectiveness of a preventive countermeasure. Preliminary conclusions derived from these tests will also be discussed in this paper.

CASE STUDY OF LATERAL FLOW IN THE FIELD

A typical example of lateral flow in a liquefied sand induced by the presence of a surcharge is the massive movement of the level ground observed in the city of Niigata at the time of the Niigata earthquake in 1964. The map of the city is shown in Fig. 1 where places of liquefaction are also indicated. A relatively small area on the north bank of the Shinano river indicated in Fig. 1 suffered destructive damage due to the massive ground flow resulting from liquefaction. The feature of the ground movement was investigated by examining a set of air photographs taken prior to and after the earthquake (Sato-kogyo, 1988). The amount and direction of the ground surface movement obtained from this analysis are indicated in the form of vector on the local map in Fig. 2, where it may be observed that there are two streams of the ground movement, one towards the river channel and the other outward from the railway

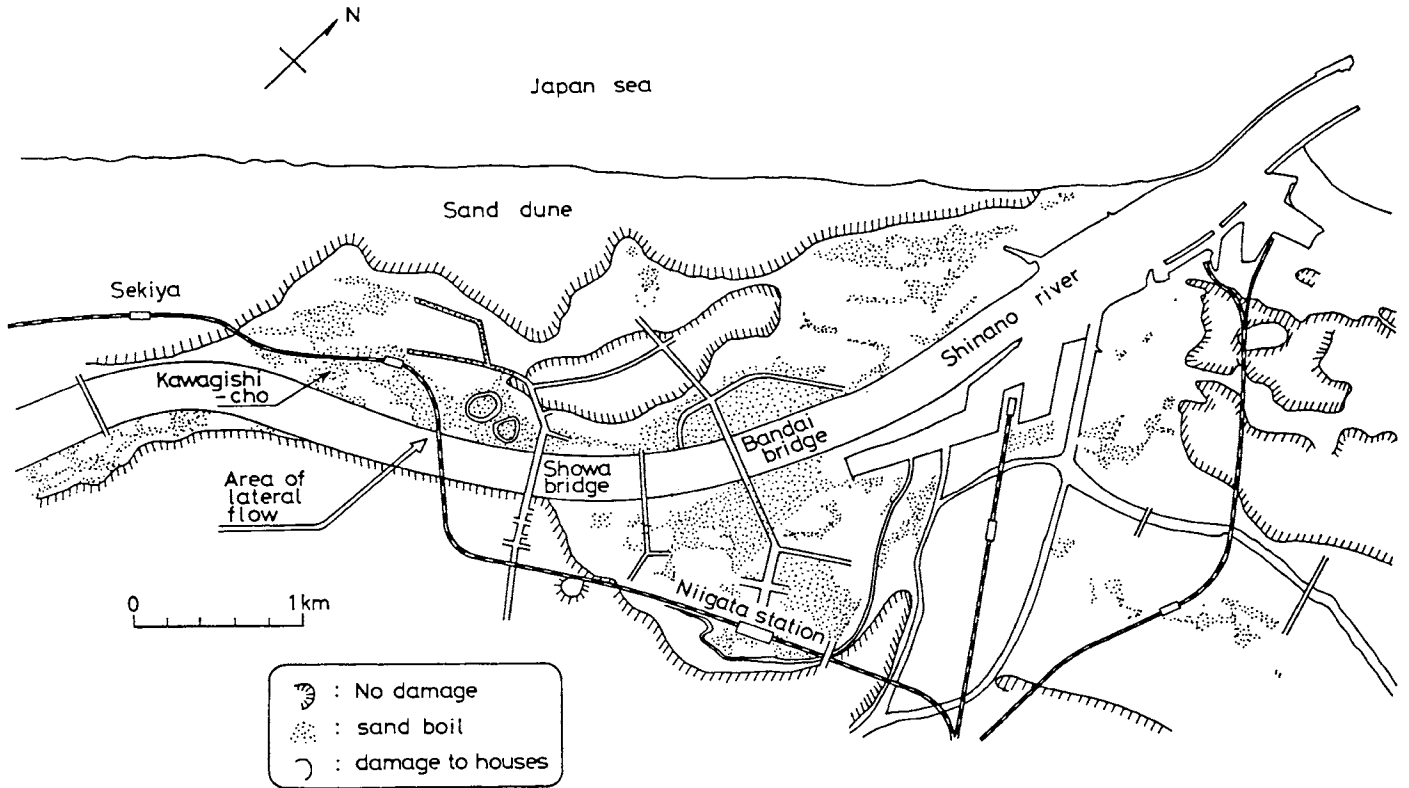


Fig. 1 Ground damage in the city of Niigata due to the 1964 earthquake.

embankment. The area south of the railway fill is seen to have moved predominantly toward the river without being influenced by the embankment, whereas the ground movement in the northeast side does possess a noticeable component in the direction perpendicular to the railway line indicating an influence exerted by the railway embankment. Thus, it may be postulated with reasons that the failure of the railway fill had taken place predominantly toward the area northeast of the fill, and a significant amount of fill materials was pushed away, thereby causing a lateral flow of the sand deposit which had been liquefied by the seismic shaking during the 1964 Niigata earthquake. The extent to which the lateral flow had spread is estimated to be approximately 150 m away from the railway line, as indicated in Fig. 2. From the observation as above, it may be mentioned that, if the ground in the surrounding area is liquefied, the influence of an embankment failure is not limited within a localized area in its vicinity but could be widespread involving a lateral flow through a distance of more than 100 m away. To put it in a more general term, it may be asserted conclusively that, while the ground failure without liquefaction in its surroundings involves a limited amount of soil mass, the failure can spread over a wide area inducing a lateral flow of soil mass, if the soil in its surroundings is liquefied due to the shaking during earthquakes.

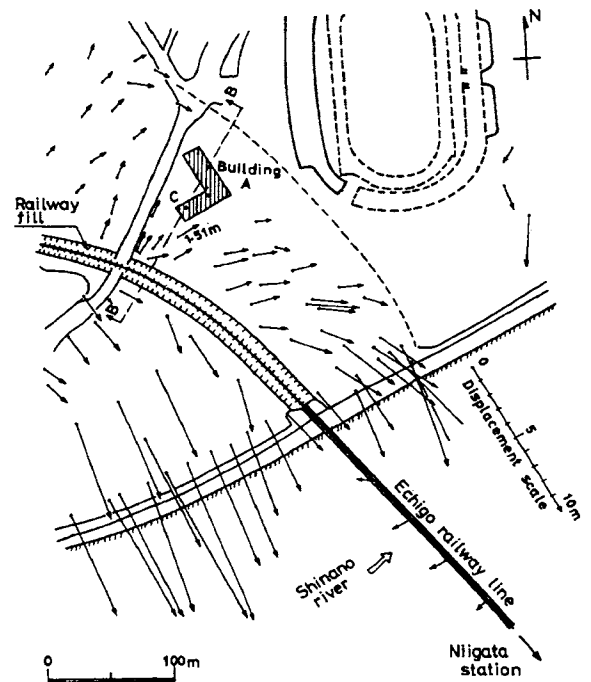


Fig. 2 Ground movement in the area of the north bank of the Shinano river.

Recently, an attempt was made by Yoshida and Hamada (1990) to investigate the damage to foundation piling during the Niigata earthquake of 1964. Excavation of two pits was carried out at a site of an old building dismantled recently. At two places where footings had existed, the ground was enclosed by driving sheet piles and the excavation was advanced to a depth of 10 m inside the sheet pile walls while the ground water was pumped up. The location of this excavation is indicated in Fig. 2. After exposing the reinforced-concrete piles 30 cm in diameter in the excavated pit, the mode of deformation and damage of the piles were carefully investigated. The outcome of this investigation disclosed the fact that the piles had deformed in the same direction as that of the ground surface determined from the air photograph analysis, and that the breakage had occurred at depths of 2 m and 7 m from the pile caps. From the deformed shape of the excavated piles, the displacement on the ground surface was estimated to be of the order of 1.5 m which is coincident with the value inferred from the air-photograph analysis. Thus, assuming the length of the lateral flow to have been 85 m from the A building site as shown in Fig. 2, the average strain on the ground surface in the direction of flow is estimated to have been approximately 1.8 %. Drilling was also performed to clarify the soil profile in the area of the pit excavation. The soil profiles obtained at two borings are shown in Fig. 3 where it may be seen that a loose deposit of clean sand exists near the surface to a depth of about 10 m. In the light of the soil profile data and the deformed shape of the excavated piles, the depth of a sliding plane at this place at the time of the 1964 event was inferred to have been probably about 7.5 m from the ground surface.

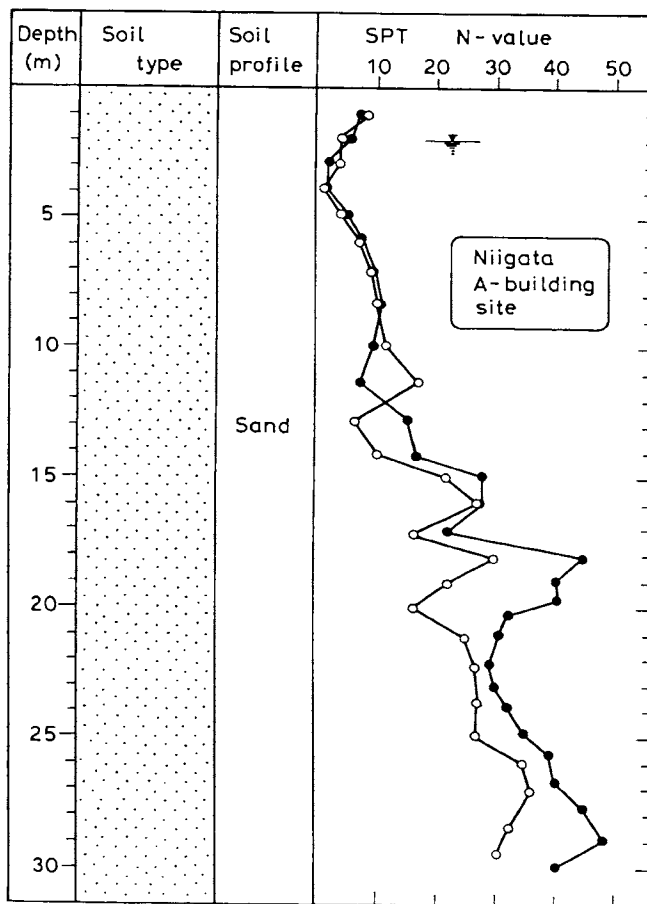


Fig. 3 Soil profile at A-building site in Niigata.

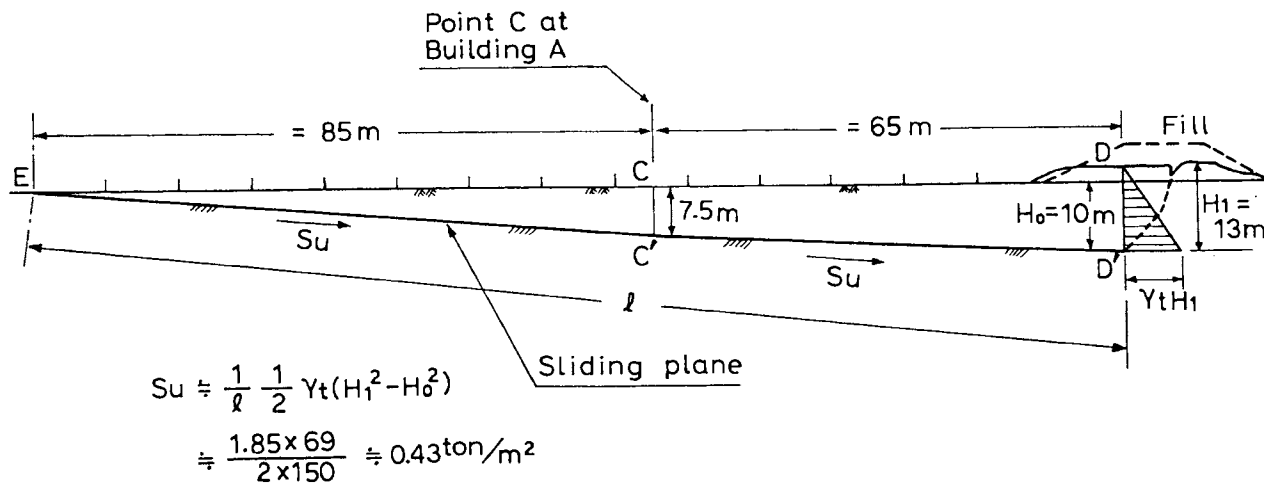


Fig. 4 Approximate location of the sliding plane in the liquefied sand deposit. (Cross section B-B' in Fig. 2)

SHAKING TABLE TESTS BY PUBLIC WORKS RESEARCH INSTITUTE

On the basis of the distance of the flow slide advancement and the liquefaction depth at point C in Fig. 2, it may be possible to assume a sliding plane which is approximated by two straight lines extending from the position of the railway embankment to a point on the ground surface about 150 m distant from the toe of the embankment. The sliding plane thus established for a typical cross section B-B' in Fig. 2 is described in Fig. 4. In view of the fact that the boring data in Fig. 3 are considered to represent a general profile of soil deposits in this area, the depth of liquefaction at the railway embankment is assumed to be 10 m. Then, the sliding plane was established by connecting points EC' and D' by two straight lines. Along the slide plane, the residual strength, S_u , is assumed to have been mobilized at the time when the lateral flow was induced. The value of the residual strength may be evaluated approximately by considering a horizontal equilibrium of forces acting on the approximate triangular section EDD' shown in Fig. 4. It is known that the original height 5 m of the railway embankment was reduced to about 3 m as a result of slumping and this slight surcharge is considered to be a source of driving force leading to the flow failure. In making a simple analysis, it is postulated that the horizontal pressure on the section DD' in the liquefied sand mass be in balance with the sum of the residual strength mobilized along the length, ℓ , of the sliding plane. As indicated in Fig. 4, the residual strength in the liquefied sand is evaluated approximately as,

$$S_u = \frac{1}{2\ell} \gamma_t (H_1^2 - H_0^2) = 0.43 \text{ ton/m}^2$$

where $\gamma_t = 1.85 \text{ ton/m}^3$ is the assumed unit weight of the liquefied sand and $H_1 = 13 \text{ m}$ is the depth of the sliding plane at point D where the slumping of the embankment took place. The residual strength estimated above is well within the range of values similarly estimated from other case studies (Ishihara et al. 1990, 1991). The values of the residual strength, longitudinal distance of lateral flow from the embankment site and the average lateral strain are listed in Table 2.

As observed in the foregoing, once liquefaction develops, large deformation or flow can occur even in the level or flat ground under the influence of a slight unbalanced driving force coming from distant objects such as embankments or buildings. One of the evidences in support of this observation would be provided by a series of large-scale shaking table tests on model soil deposits conducted by the Public Works Research Institute (Sasaki et al. 1991). In the general arrangements of these tests, loose saturated deposits of sand with a relative density of 50 % was provided with different thickness in a 6 m long, 0.8 m wide and 2.0 m high test box. In one of the tests in the series (Model 6) a gently sloped surcharge consisting of shots of lead and gravel was placed over one half length of this deposit. The test arrangements quoted from the paper by Sasaki et al. (1991) is shown in Fig. 5.

The surcharge on the right side had a slope of 5 % and the layer of sand to a depth of 35 cm was placed loose enough to generate liquefaction in each step of table shaking. The shaking was applied to the table in four sequences each with stepwise increased horizontal acceleration from 60 to 190 gals. The acceleration had a sinusoidal wave form. The pattern of horizontal deformation in step 2 after 20 seconds of continued application of shaking with an acceleration of 104 gal is demonstrated in Fig. 6(a). The picture of deformation was established from observed displacements of strips of colored sand placed on the transparent glass window. The glass window was installed only through the 4 m portion in the middle of the box. It may be seen that the sliding surface tends to develop shallower toward downstream, probably because of the rigid constraint on the end of the box. Although invisible, it may well be assumed that the depth of sliding surface becomes gradually shallower coming up on the surface at the left end. The depth of the sliding plane on the right end may be assumed to extend to the bottom of the liquefied layer.

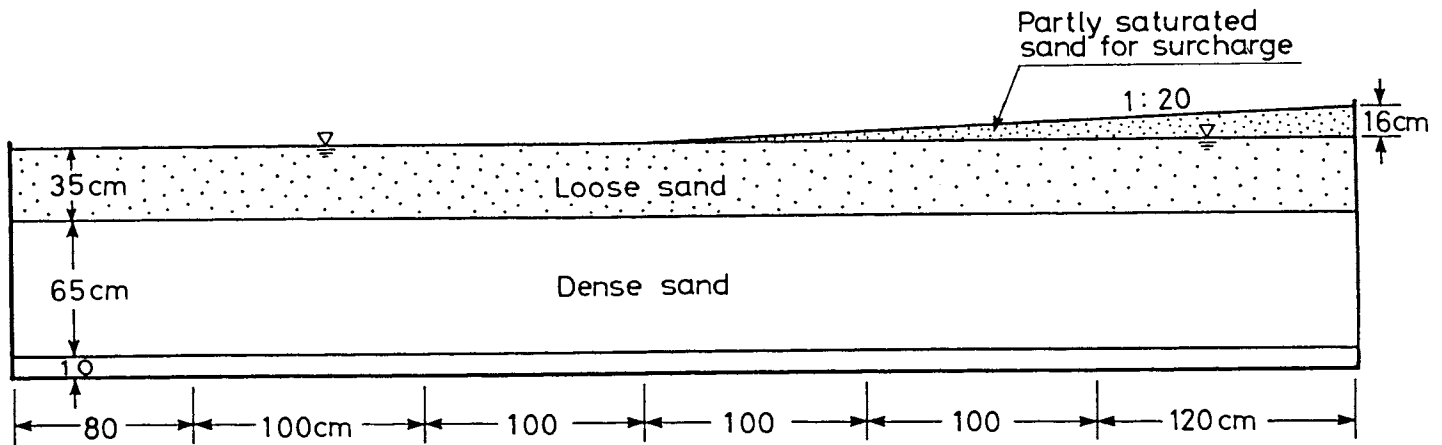


Fig. 5 Test arrangement for Model-6 by PWRI (Sasaki et al. 1990).

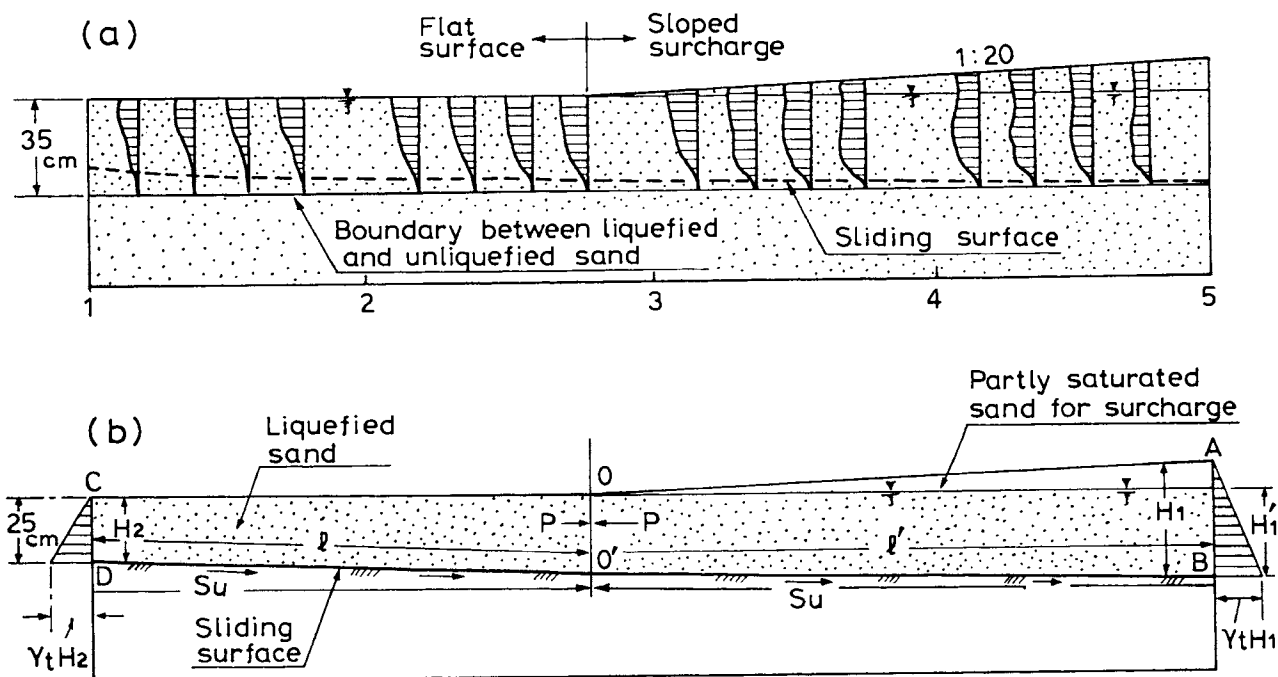


Fig. 6 Pattern of lateral deformation and scheme of simple analysis in PWRI tests.

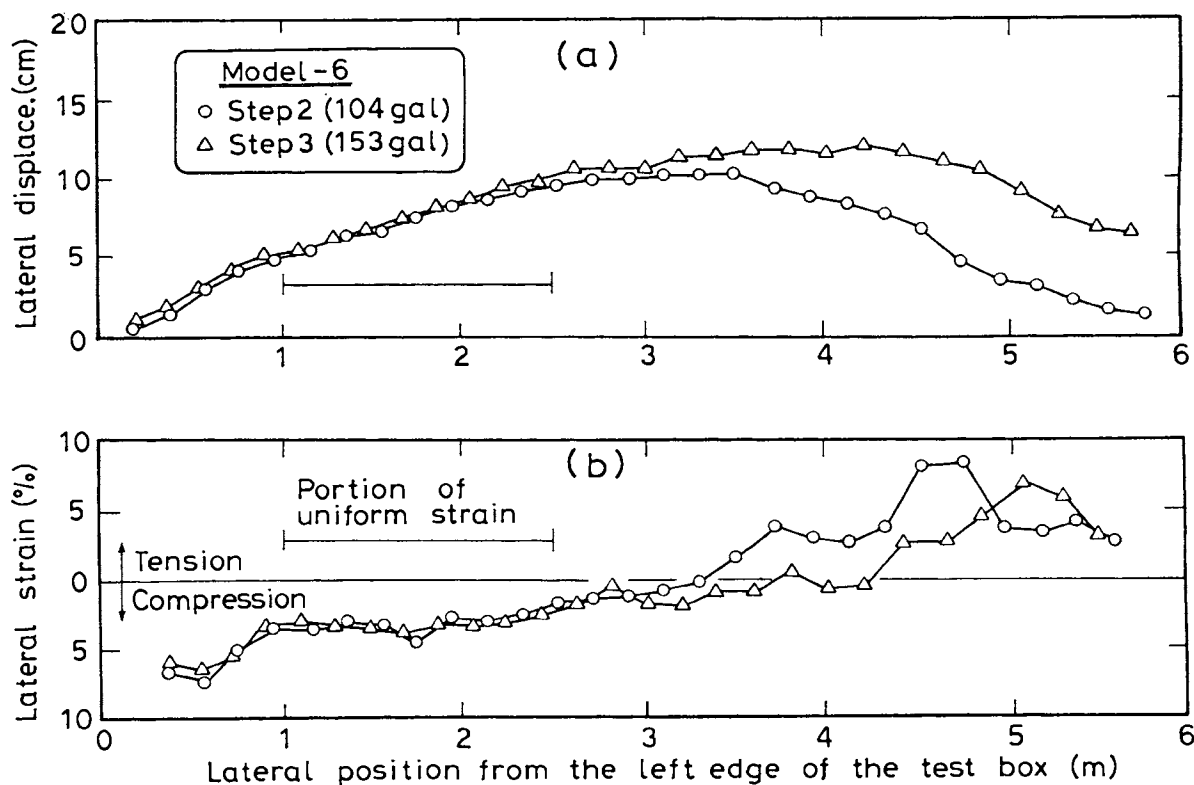


Fig. 7 Lateral deformation of the ground surface observed in the tests by PWRI (Sasaki et al. 1991).

At the time the flow was under progress, the presence of the surcharge on the right side was a source of driving force causing the lateral deformation in the liquefied sand deposit. Thus, assuming a sliding surface as indicated by DO'B in Fig. 6(b), a force equilibrium can be established and the residual strength is calculated as,

$$S_u = \frac{1}{(\ell + \ell')} \frac{1}{2} \gamma_t (H_1 + H_2) (H_1' - H_1) \dots (1)$$

Introducing a set of properly assumed values of $\ell' = 2.2$ m, $\ell = 1.8$ m, $\gamma_t = 1.85$ t/m³, $H_1 = 0.51$ m and $H_2 = 0.25$ m, $H_1' = 0.35$ m the residual strength is estimated roughly as,

$$S_u = \frac{1.85}{4 \times 2} \times 0.76 \times 0.16 = 0.028 \text{ ton/m}^2$$

The horizontal displacement of the ground surface in the longitudinal direction measured by a set of markers placed on the fill is demonstrated in Fig. 7(a) for two steps of shaking application. It may be seen that, the lateral deformation tends to decrease leftwards from the toe of the fill in the middle, becoming equal to zero at the left end of the fill. On the right-hand side where there is the surcharge, the lateral displacement tends to decrease rightwards but not in a consistent manner. The lateral strain on the ground surface in the longitudinal direction was obtained on the basis of the displacement measurements as described above, and demonstrated in Fig. 7(b). Looking at the overall picture of strain distribution, one can clearly recognize that the surface of the surcharge fill on the right half underwent tensile-strains, whereas compressive strains were produced on the surface on the left half portion of the model deposit. In order to examine the characteristics of flow-type deformation induced by liquefaction, it will be preferable to draw attention to the longitudinal strains in the middle of the flat portion of the deposit where the strain development is uniform, not being influenced by the surcharge on the right side and free from the constraint by the rigid wall on the left end. Such a strain appears to have been produced in the 1.5 m-long portion of the model deposit as indicated accordingly in Fig. 7(b). The uniformity in the strain in this portion may be recognized by looking at the distribution of the lateral

deformation in the corresponding part in Fig. 7(a). From Fig. 7(b), the average value of longitudinal compressive strain may be read off as being about 3.5%. The values of the back-calculated residual strength and average lateral strain are listed in Table 2. From the above observation, it may be mentioned that the lateral flow in a uniformly liquefied sand deposit takes place in such a way that the horizontal displacement on the ground surface decreases linearly with increasing distance from the place where the flow is originated. In other words, the lateral flow occurs so that the strain in the direction of flow is maintained at a constant value. It appears difficult to quantify the magnitude of the lateral strain itself, because it is a value to be determined from the length of flow and the lateral displacement of the ground at the place of flow outset.

SHAKING TABLE TESTS BY OKUMURA CO.

A series of shaking table tests was conducted in the laboratory of Okumura Co. to observe the occurrence of liquefaction and consequent flow-type deformation, if it occurs, in loose deposits of sand. A large box 4.5 m long, 0.9 m high and 2 m wide with transparent lucite-made side walls was placed on a shaking table having a maximum dynamic load capacity of 60 ton with 1 g acceleration, as shown in Fig. 8. At one end of the bin, a rigid steel plate was bolt-fixed to provide an inclined boundary for minimizing the adverse effects of end constraint which may inhibit the smooth continuous deformation of sand deposits through the length of the box. Sand from Sengenyama in Chiba was used to provide loose sediments of sand. The grain size characteristics of the sand is shown in Fig. 9 where it is seen that the mean diameter, D_{50} , is 0.30 mm. To construct a model dike on top of the sand deposit, a clayey silt material was prepared by blending cement, kaolinite and feleit with 1 : 2 : 1.5 proportion in weight. Owing to a heavy-weight feleit material, the unit weight of the dike material was as much as 3.0 ton/m³.

The test bin was pooled with water and then the dry sand was rained through a narrow slit of a sliding hopper atop the box. By this procedure, a uniform sand deposit was obtained with a relative density of 40%. In some tests where it was necessary to provide a compacted zone, two steel plates were first placed

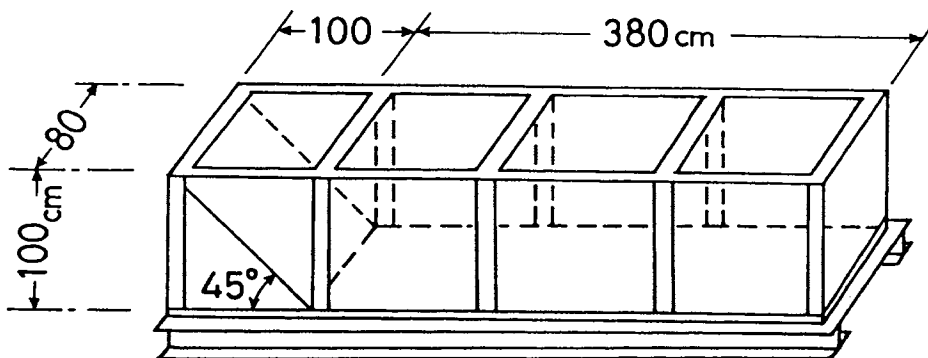


Fig. 8 Test box used in the tests by Okumura Co.

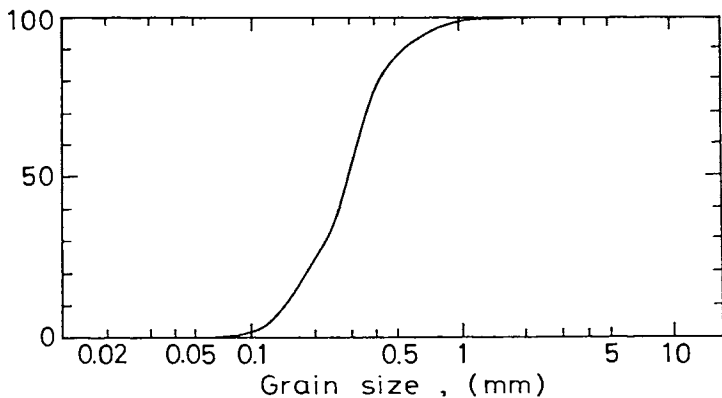


Fig. 9 Grain size distribution curve of Sengenyama sand.

vertically across the test bin to provide an enclosure and the sand was poured from the hopper. Every time the sand was piled up about 10 cm, the loose deposit enclosed within these two steel plates was compacted with a rammer and then the plates were pulled up by about 10 cm. By repeating this procedure successively, a compacted zone with a relative density of 80 % was provided in the middle portion of the test bin.

To facilitate visual observation of deformation progress in the sand deposit, a lattice of white-colored sand was provided on the face of the transparent front wall.

At each stage of the sand placement as above, sets of piezometers and accelerometers were installed at pre-determined locations within the fill. After completing the sand filling, a 30 cm high model dike with a frontal slope 1 : 2.5 was placed at one end of the deposit. The water table was maintained at the level of the ground surface. The displacement gauges were then placed on the surface along the center line of the model dike and the deposit.

In all the tests, the test bin was shaken by a sinusoidal motion with a frequency of 2Hz having an acceleration amplitude of 200 gal. The shaking was continued as long as necessary until the model deposit and dike have deformed significantly.

Test with Uniform Sand Deposit

The first in the series was a test in which the model dike was placed on a uniform deposit of loose sand with a relative density of 40 %. The test arrangements are schematically described in Fig. 10(a). Exact locations of pickups for acceleration and piezometers are shown in Fig. 11. Time histories of pore water pressures monitored at key points along the mid-depth of the model fill are presented in Fig. 12. It may be observed that the pore water pressures at P 57 and P 63 distant from the dike

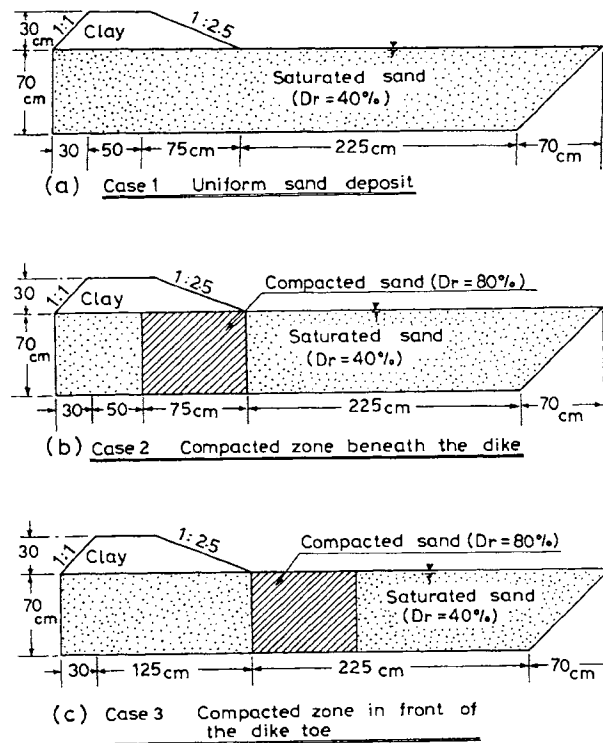
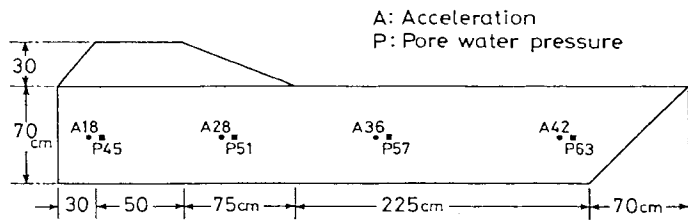


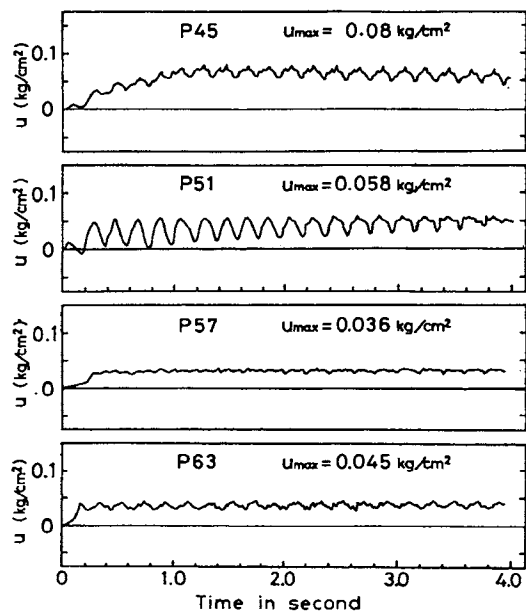
Fig. 10 Layouts of the sand deposits for the shaking table tests.

indicated a sharp rise to a level of initial overburden pressure within the first one and half cycles, whereas there was some delay in the pore pressure build up at P 45 and P 51 located in the vicinity of the dike. Time histories of accelerations recorded at key points within the model fill are presented in Fig. 13. It may be seen that at locations P 36 and P 42 distant away from the dike the acceleration drops sharply after one and half cycles of shaking, whereas similar drops in acceleration occurred 2 to 3 cycles later at point A 18 located beneath the dike. The characteristic change in acceleration in harmony with the pore water pressures as above indicates the fact that the liquefaction developed first in the portion of the sand deposit free from any constraint of the dike and then progressed to the deposit near the dike where the resistance to liquefaction was stronger owing to the sustained shear stress produced by the surcharge of the dike. Vertical displacements monitored along the surface of the dike and fill showed that, while the dike and its toe settled, the free field portion away from the dike experienced a heave on the order of 20 to 50 mm. The pattern of deformation obtained from the visual observation of the latticed white-colored sand is demonstrated in Fig. 14(a) for the final stage where the dike completely slumped accompanied with large lateral deformation. It is to be noticed here that the lateral deformation and heave has progressed through a long distance away from the toe of the dike. This observation is indicative of the fact that the influence of a driving force caused by the presence of an object such as dikes and buildings on the liquefied level ground could spread farther out and create a large-scale lateral flow of the liquefied sand.



(a) Case 1 Uniform sand deposit

Fig. 11 Locations of pickups.



Case 1 Uniform sand deposit

Fig. 12 Monitored pore water pressures.

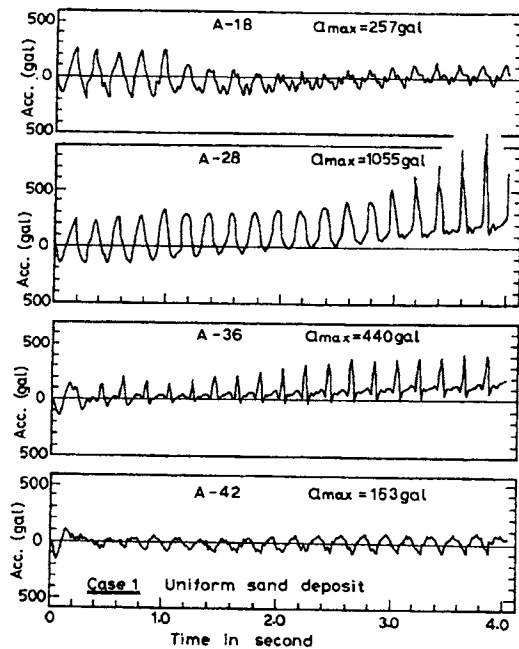
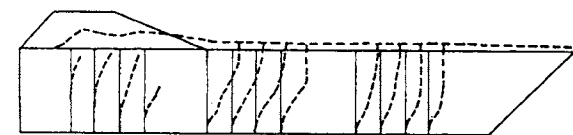
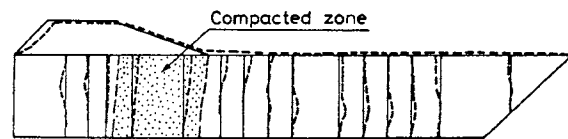


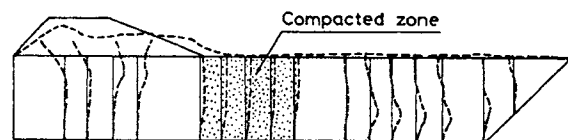
Fig. 13 Monitored accelerations.



(a) Case 1 Uniform sand deposit



(b) Case 2 Compacted zone beneath the dike



(c) Case 3 Compacted zone in front of the dike toe

Fig. 14 Patterns of permanent deformation after the tests have finished.

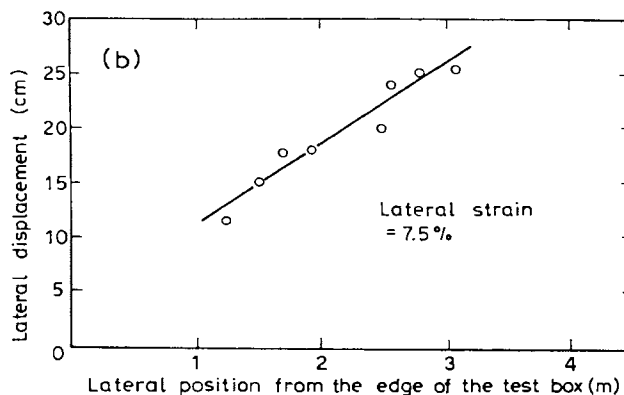
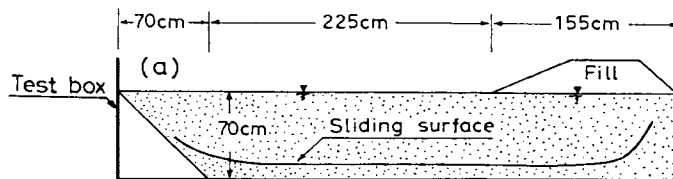


Fig. 15 Sliding surface and lateral displacements.

By assuming an approximate tri-linear sliding surface as shown in Fig. 15(a), a stability analysis was made to back-calculate the residual strength of the liquefied sand which appears to have been mobilized along the horizontal portion of the sliding plane in the middle. In this analysis, the static driving force was estimated by considering the completely slumped configuration of the model dike. This force minus the counter-acting force

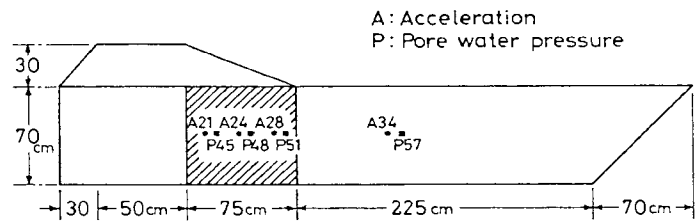
on the other end was divided by the distance of the horizontal portion of the sliding plane. The residual strength thus calculated was 0.05 ton/m^2 , which was small enough to induce the flow structure of any liquefied sand. The development of horizontal displacement on the surface was also monitored by a set of markers in the series of the shaking table tests conducted by Okumura Co. In the case of the test in which a uniform sand deposit was shaken to generate liquefaction, the horizontal deformation at the end of the shaking was distributed, as shown in Fig. 15(b), through the length of the model deposit. The characteristic uniform deformation neither affected by the end constraint nor by the surcharge is considered to have taken place in the middle of the flat portion, as indicated in Fig. 15. Thus, by reading off the slope in the deformation versus distance plot, the compressive strain in the longitudinal direction on the surface is determined to be approximately 7.5 %.

Test with Compacted Zone Beneath the Dike

The second test in the series was identical to the first one except for the provision of a compacted zone beneath the slope of the dike. The dense sand zone 75 cm wide compacted to a relative density of 80 % is shown in Fig. 10(b). Exact locations of the acceleration pickups and piezometers are shown in Fig. 16. The pore water pressures monitored at four locations along the mid-depth of the deposit are displayed in Fig. 17, where it may be seen that the buildup of pore pressures was significantly small and slow at points P 45 and P 48 within the compacted zone, in contrast to the immediate buildup at point P 57 in the uncompacted loose part far from the dike. The corresponding records of accelerations are shown in Fig. 18 which indicate that near the compacted zone the acceleration keeps on its initial level, but it drops sharply at a place far from the dike where a rapid decline in rigidity is encountered due to the pore pressure buildup. The settlement records on the surface indicated that the amount of settlement is one order of magnitude smaller as compared to that in the previous test without compacted zone. The loose zone outside the compacted zone appears to have behaved on its own characteristics without being influenced by the dike. The configuration of the dike-deposit system after the start of shaking and at a final stage where deformation has ceased to develop are displayed in Fig. 14(b). With the crest settlement as small as 22 mm and without any spread of lateral deformation toward the loose zone in front of the dike toe, it may be mentioned that the compacted zone, being properly positioned, acted most effectively toward reducing the distress caused by the excessive lateral deformation of the loose sand deposit which would otherwise had occurred as evidenced by the first test in the series.

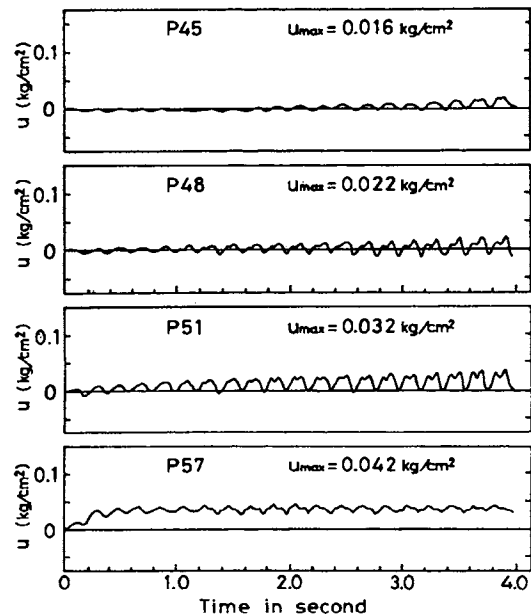
Test with Compacted Zone in Front of the Dike Toe

As the third in the series, a test was conducted in which a compacted zone was provided in the deposit in front of the dike toe as shown



(b) Case 2 Compacted zone beneath the dike

Fig. 16 Locations of pickups.



Case 2 Compacted zone beneath the dike

Fig. 17 Monitored pore water pressures.

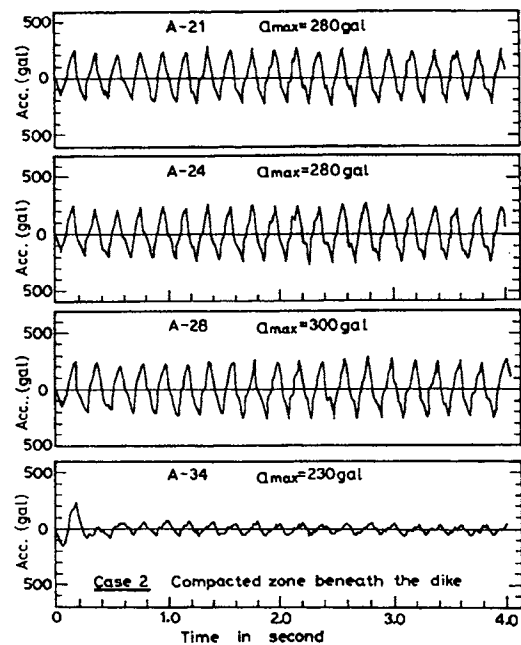
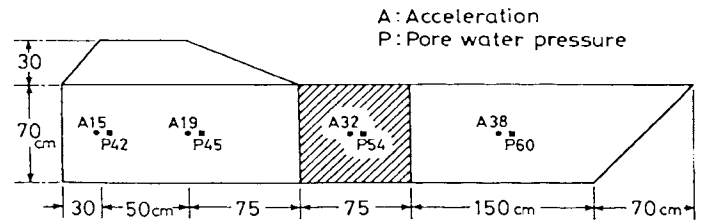


Fig. 18 Monitored accelerations.

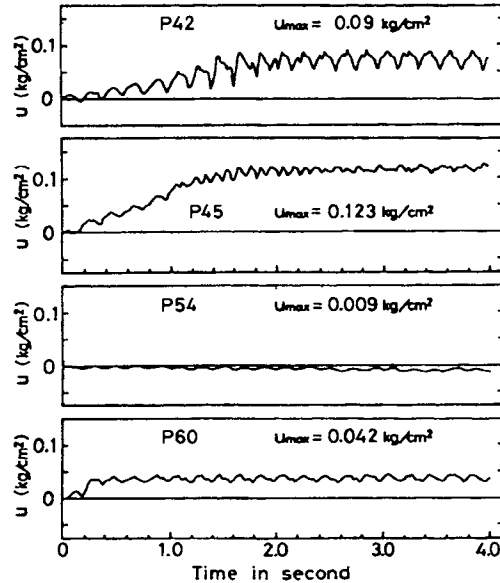
in Fig. 10(c). Other conditions were identical to those in the previous two tests except for this shift in the location of the compacted zone. The locations of the pickups for acceleration and pore water pressure measurements are indicated in Fig. 19. The pore pressures monitored during the shaking at four representative spots are displayed in Fig. 20. It may be observed that the piezometer at P 45 in the loose zone below the dike indicated a sharp rise in the early part of the shaking. Similar rapid buildup of pore pressures was also recorded in the loose zone far away from the dike. In contrast to this, the piezometer within the compacted zone indicated native pore pressures, because of the dilatant tendency of the dense sand by the shear stress generated by the weight of the dike. The acceleration records at point A 38 in Fig. 21 showed a sudden drop in amplitude corresponding to the sharp rise in pore pressure at this location. The acceleration within the compacted zone showed practically no change in its amplitude, indicating that the rigidity of the sand in this zone had remained unchanged. The measured settlements of the dike crest was on the order of 80 to 125 mm which is a fairly large amount as compared to 22 mm observed in the second test. In contrast to this, the settlements away from the dike were much smaller. The overall configuration at the final stage are demonstrated in Fig. 14(c). It may be seen that, while the compacted part did not move appreciably, the dike settled significantly. In fact, severe cracking near the toe of the dike slope was seen developing at the end of the shaking where the liquefied sand and water oozed or spurted out of the loose zone beneath the dike. It appears that the pore pressures developed under the dike pushed up the portion of small surcharge and broke out the toe expelling the liquefied sand. The amount of the dike settlement was equal to the volume of water and sand which had been expelled out of the underlying liquefied zone. The observation as above thus appears to indicate that, if the surcharge is not thick enough, there remains a high possibility for the underlying liquefied sand coming out on the surface, thereby causing destruction due to intolerable settlements of the dike. It is obvious that the presence of the compacted zone had acted favorably as a stopper to prevent a complete slumping of the dike due to the lateral flow of the liquefied sand. In this sense, some beneficial effects could be expected from the installation of a compacted zone, but at a sacrifice of an adverse consequence as described above. Thus, it may be mentioned that the installation of a compacted zone would be completely effective only when it is executed in front of a liquefiable zone which is covered by a sufficiently thick surcharge. Installing a compaction zone just beneath the dike such as that executed in the second test satisfies this requirement and hence successfully achieved an intended purpose in minimizing the crest settlement.

The characteristic features observed in the three model tests using a large shaking table are summarized in Table 1.



(c) Case 3 Compacted zone in front of the dike toe

Fig. 19 Locations of pickups.



Case 3 Compacted zone in front of the dike toe

Fig. 20 Monitored pore water pressures.

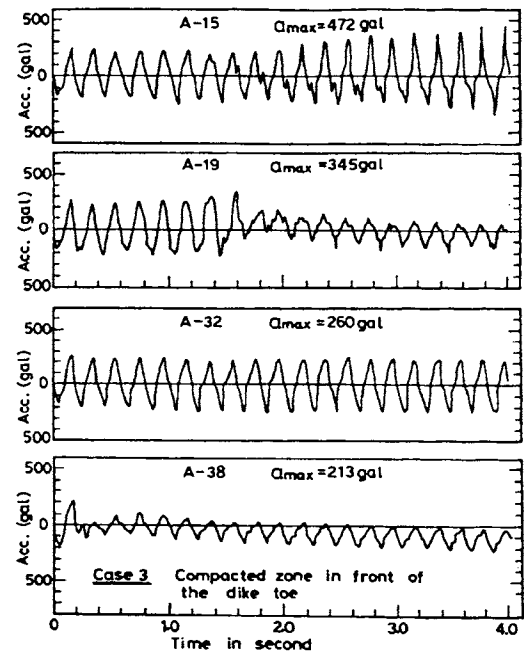





Fig. 21 Monitored accelerations.

Table 1 Characteristic features of three model tests

Type of model test	Characteristic phenomena	Crest settlement	Schematic picture of test arrangements
Test with uniform sand deposit	Lateral flow of liquefied sand with complete dike slumping	$0.67H^*$ = 200 mm	
Test with compacted zone beneath the dike	Tolerably small dike settlement with no lateral flow	$0.07H$ = 22 mm	
Test with compacted zone in front of the dike	No lateral flow but breach in the dike toe with some settlement	$0.41H$ = 125 mm	

*H: height of the dike (= 300 mm)

CONSIDERATIONS FOR FLOW SLIDE

In the foregoing sections, performances of liquefied sand deposits both in the field and in the laboratory were introduced and discussed in the same context, and almost similar behavior was observed, irrespective of whether it is in the field or in the laboratory. But there seems to be one big difference between them. That is the behavior after cessation of the shaking. In all of the model tests on shaking tables including the two as above, the deformations or flow have been observed to progress only when the shaking was underway, and the movements stopped almost suddenly when the shaking was terminated. On the other hand, there have been a number of reported field evidences by eyewitnesses who attested that a large part of the deformation such as settlements of buildings and lateral ground movements took place in a quiet period after the shaking by earthquakes had stopped. There may be several reasons conceivable for explaining this difference. There seems to be two factors influencing the occurrence or non-occurrence of the large deformation after the cessation of the shaking. One factor would be the difference in the length of time required to bring about the deformation in a mass of soils with different sizes. It is most likely that in small-sized models on the shaking table the deformation of liquefied sand can occur quickly within a matter of several seconds, whereas it takes a longer time of the order of several minutes for a more massive in-situ soils to move. Thus, the larger the mass of soils, the longer the duration of time required for the deformation of a soil mass to occur. Another conceivable factor would be the decrease of the residual strength during the application of shaking. Although this issue has not been addressed explicitly, it is highly likely that the residual strength under an action of vibration is smaller than that mobilized under a quiet condition without shaking.

With these two factors combined together, the scenario of deformation occurrence in the model on the shaking table may be envisaged as follows. In many of the model tests in the laboratory, a shaking with uniform amplitude is applied from the beginning so that onset of liquefaction with 100 % pore water pressure buildup can be achieved relatively quickly within a matter of several cycles, but the shaking is continued further until seizable amount of deformation is induced. Thus, during the period of time following the onset of liquefaction, the sand in the model is put in a steady state with a smaller residual strength under the action of vibration and hence the model tends to deform more largely than if it is allowed to under a quiet condition without shaking. The model is small enough in size to be able to fully deform as quickly as it can within the short period of time. Therefore, when the shaking is stopped and a normal steady-state prevails, the corresponding residual strength becomes greater and the sand in the model can not deform any farther. In other words, the model on the shaking table has already deformed excessively matching the low residual strength under shaking and the driving force resulting from the largely deformed or slumped surcharge becomes no longer great enough to generate further deformation under the increased residual strength without any shaking. In contrast to this, the liquefaction in the field is known to occur at a later stage of the main shaking lasting about 10 to 40 seconds, and there is practically no time for the sand undergoing any shaking while it is in a steady-state. Thus, most of the deformation in in-situ deposits of sands appears to take place under the normal conditions of steady-state without shaking. Since large masses of sands in the field take longer time to be displaced, the flow failure in-situ does develop slowly after the cessation of the shaking during earthquakes.

Table 2 Key parameters associated with flow slide

Cases	Length of lateral flow (m)	Depth of liq. at outset point H_0 (m)	Lateral displace at outset point U_0 (m)	Average lateral (%)	Residual strength S_u (ton/m ²)
Building A site in Niigata	150	7.5	1.5	1.8	0.43
Model test by PWRI*	Full length is not known	0.3	0.1	3.5	0.028
Model test by Okumura Co.	Full length is not known	0.6	0.25	7.5	0.05

*Public Works Research Institute

SIMPLE ANALYSIS OF FLOW SLIDE

In the foregoing sections, simple analyses have been made for each case of the field and laboratory studies to back-calculate the residual strength mobilized in the liquefied deposits of sands during the lateral flow. The values of the residual strength thus obtained are summarized in Table 2. In the case of the shaking table tests in the laboratory, the value of residual strength is shown to be one order of magnitude smaller than that obtained from the field performance data. This difference appears to have emerged mainly from the fact that the sands in the laboratory tests have deformed during the application of shaking and hence, as explained in the foregoing section, under a steady-state in which the mobilized residual strength was smaller than that in a quiet condition.

Many efforts have been made in recent years to investigate the residual strength of once liquefied sands and silty sands (Castro; 1975, 1977; Seed, 1987; Ishihara et al. 1990; Marcuson et al. 1990). The outcome of these studies has indicated that the residual strength of sand in its largely deformed state can take a value as large as 3 to 5 ton/m² and also a value as small as 0.01 ton/m², depending upon the type and density of the sand, but in many cases investigated the residual strength in the field deposits is known to show a value ranging between 0.1 and 2.0 ton/m², which is approximately coincident with the value obtained from the present study of the Niigata site as shown in Table 2.

In the design and practice of buried pipe lines and underground structures, it will be necessary to have a methodology by which to estimate the extent of flow failure advancement and the amount of associated ground deformation that can develop in the level ground in front of some surcharge objects such as dikes and embankments. For such a case, a simple analysis

may be developed, as follows, on the basis of some assumptions derived from the considerations in the foregoing sections.

(1) First of all, based on the conventional method, liquefaction analysis is performed for a given sand deposit under consideration, and the depth of liquefaction is determined. At the same time, the surcharge pressure such as a height of dikes after slumping must be assessed by an appropriate procedure. The depth of liquefaction plus the height of the surcharge will specify the depth, H_0 , through which the lateral driving force acts to generate the flow slide, as illustrated in Fig. 22.

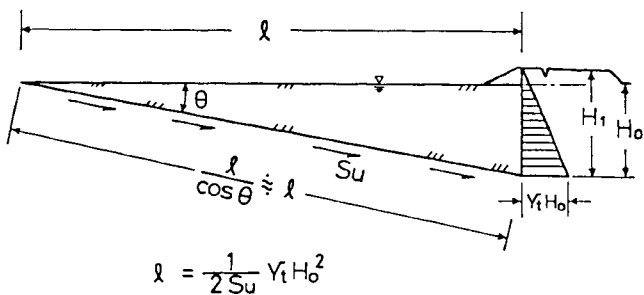
(2) The next step consists in evaluating the residual strength, S_u , that can be mobilized in the liquefied sand deposit. Although somewhat difficult in the present state-of-the-art, an approximate value needs to be assessed by one way or another.

(3) By assuming the sliding plane to be represented by a straight line as illustrated in Fig. 21(a), its length, ℓ , can be determined from the equilibrium condition as follows,

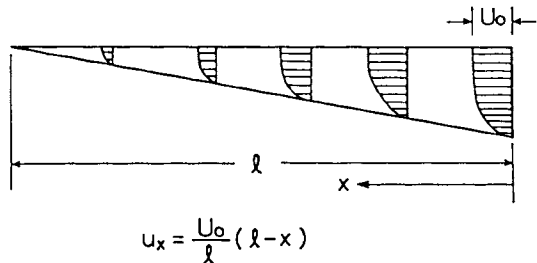
$$\ell = \frac{1}{2S_u} \gamma_t (H_1^2 - H_0^2) \quad \dots (2)$$

where γ_t is the unit weight of the liquefied sand.

(4) The next step is to estimate the amount of lateral displacement, U_0 at a point where the flow is initiated. This displacement will depend mainly on the amount of slumping which may be dependent in turn on the soil type composing the fills and also on the duration of seismic shaking. Although difficult to quantify these factors, the displacement, U_0 , must be assessed by some appropriate procedures or judgements based on past experiences.



(a) Force equilibrium



(b) Lateral deformation based on the uniformity of lateral strain

Fig. 22 Scheme of simple analysis.

(5) The amount of displacement at a given place on the surface of the liquefied ground can be determined on the basis of the uniformity postulate of lateral strain derived from the shaking table tests as mentioned above. As illustrated in Fig. 21(b), the displacement, U_x , at a point x , is determined from,

$$U_x = \frac{U_0}{l} (l-x) \quad \dots \dots (3)$$

CONCLUSIONS

Brief review was made over the results of two series of large-scale shaking table tests in the laboratory performed recently for investigating the mechanism of flow failure which occurs in the sand deposit following the outset of liquefaction during earthquakes. The model tests in the laboratory have clearly demonstrated that a flow type deformation could occur and advance through a long distance in the flat ground in front of a surcharge such as dikes and embankments. The long-distance progress of the flow failure was also shown to have developed in the field at the time of the 1964 Niigata earthquake. As a result of the observation of laboratory performances of liquefied sand deposits, it was discovered that the compressive lateral strain on the ground in the direction of flow is uniform throughout the area involved in the flow. The results of simple analysis have also revealed that the residual strength mobilized during the flow was in the same range as that suggested from other investigations. On the basis of the assumption for the sliding plane being a straight line and also on the uniformity postulate of the lateral

strain, a simple method of analysis was proposed to assess the amount of lateral deformation which can develop in the liquefied ground under the action of a driving force produced by a surcharge such as dikes and embankments.

In a series of the large-scale shaking table tests conducted by Okumura Co., efforts were made to find out an effective measure to prevent the progression of the flow slide in front of the dike. As a corollary of this studies, provision of a compacted zone beneath the dike was shown to be an effective countermeasure to preserve the integrity of the dike.

ACKNOWLEDGEMENTS

In preparing the manuscript of this paper, the overall cooperation by Mr. S. Yanagihara of Okumura Co. and Mr. N. Yoshida of Sato Kogyo Co. was very much helpful. Mr. K. Tokida of Public Works Research Institute kindly offered useful comments on the results of their tests. The authors wish to express their sincere gratitude to these persons.

REFERENCES

Arulanandan, K., Yagachandran, C., Muraleetharan, M.M., Kutter, B.L. and Chang, G.S. (1988), "Seismically Induced Flow Slide on Centrifuge," ASCE, Vol. 114, No. 12, PP. 1442-1449.

Castro, G. (1975), "Liquefaction and Cyclic Mobility of Saturated Sand," ASCE, Vol. 101, GT 6, PP. 551-569.

Castro, G. and Poulos, S. (1977), "Factors Affecting Liquefaction and Cyclic Mobility," ASCE, Vol. 103, GT 6, PP. 501-516.

Hamada, M., Yasuda, S., Isoyama, R. and Emoto, K. (1986), "Observation of Permanent Ground Displacements Induced by Soil Liquefaction," Proc. Japan Society of Civil Engineers, No. 336, III-6, PP. 211-220.

Hamada, M., Wakamatsu, K. and Yasuda, S. (1989), "Liquefaction-Induced Ground Displacement during the 1948 Fukui Earthquake," Proc. 2nd U.S.-Japan Workshop on Liquefaction, Large Ground Deformation, and Their Effects on Lifeline Facilities, Niagara Falls.

Ishihara, K., Yasuda, S. and Yoshida, Y. (1990), "Liquefaction-Induced Flow Failure of Embankments and Residual Strength of Silty Sands," Soils and Foundations, Vol. 30, No. 3, PP. 69-80.

Ishihara, K., Okusa, S., Oyagi, N., and Ischuk, A. (1991), "Liquefaction-Induced Flow Slide in the Collapsible Loess Deposit in Soviet Tajik," Submitted to Soils and Foundations.

Marcuson, W.F., Hynes, M.E. and Franklin, A.G. (1990), "Evaluation and Use of Residual Strength in Seismic Safety Analysis of

Embankments," Earthquake Spectra.

O'Rourke, T.D., Roth, B.L. and Hamada, M. (1989), "A Case Study of Large Ground Deformation during the 1971 San Fernando Earthquake," Proc. 2nd U.S.-Japan Workshop on Liquefaction, Large ground Deformation, and Their Effects on Lifeline Facilities, Niagara Falls.

Sasaki, Y., Tokida, K., Matsumoto, H., and Saya, S. (1991), "Experimental Study on Lateral Flow of Ground due to Soil Liquefaction," Proc. 2nd International Conference on Recent Advances in Geotechnical Earthquake Engineering and Soil Dynamics, St. Louis.

Sato Kogyo Co. (1988), "Investigation on the Damage to Pile Foundation in A-Building," Report of Association for the Development of the Earthquake Prediction.

Seed, H.B. (1987), "Design Problems in Soil Liquefaction," ASCE, Vol.113, No.8, PP. 827-845.

Wakamatsu, K., Hamada, M., Yasuda, S. and Morimoto, I. (1989), "Liquefaction Induced Ground Displacement during the 1923 Kanto Earthquake," Proc. 2nd U.S.-Japan Workshop on Liquefaction, Large Ground Deformation, and Their Effects on Lifeline Facilities, Niagara Falls.

Yoshida, N. and Hamada, M. (1990), "Analysis of Damages of Foundation Piles due to Liquefaction-Induced Permanent Ground Displacements," Proc. 8th Japan Earthquake Engineering Symposium.